Drug Binding by Calmodulin: Crystal Structure of a Calmodulin−Trifluoperazine Complex[†,‡]

William J. Cook,[*,§,||] Leigh J. Walter,[||] and Mark R. Walter[||,⊥]

Departments of Pathology and Pharmacology and Center for Macromolecular Crystallography, University of Alabama at Birmingham, Birmingham, Alabama 35294

Received July 19, 1994; Revised Manuscript Received October 18, 1994[⊗]

ABSTRACT: The crystal structure of calmodulin (CaM) bound to trifluoperazine (TFP) has been determined and refined to a resolution of 2.45 Å. Only one TFP is bound to CaM, but that is sufficient to cause distortion of the central α-helix and juxtaposition of the N- and C-terminal domains similar to that seen in CaM−polypeptide complexes. The drug makes extensive contacts with residues in the C-terminal domain of CaM but only a few contacts with one residue in the N-terminal domain. The structure suggests that substrate binding to the C-terminal domain is sufficient to cause the conformational changes in calmodulin that lead to activation of its targets.

Calmodulin is a major intracellular Ca^{2+} receptor that is present in all eukaryotic cells and mediates a variety of physiological processes in a calcium-dependent manner (Klee & Vanaman, 1982; Means *et al.*, 1991). Binding of Ca^{2+} induces marked conformational changes in CaM,[1] including the exposure of hydrophobic clefts, which are important in the binding of CaM inhibitors and target enzymes (LaPorte *et al.*, 1980; Tanaka & Hidaka, 1980). The crystal structure of Ca^{2+}−CaM showed a dumbbell-shaped molecule with two similar globular domains connected by an eight-turn central α-helix (Babu *et al.*, 1988). Each globular end possesses a hydrophobic core that is accessible to solvent along the surface facing the long helix. Recent NMR and X-ray structure determinations of CaM complexed with peptide fragments of skeletal muscle myosin light chain kinase (skMLCK) (Ikura *et al.*, 1992), smooth muscle myosin light chain kinase (smMLCK) (Meador *et al.*, 1992), and CaM-dependent protein kinase IIα (Meador *et al.*, 1993) have provided insight into the nature of CaM−enzyme interactions. These studies showed that the central helix is highly flexible and bends to allow the hydrophobic regions at each end of the molecule to interact with enzymes. The interaction of CaM with enzymes is inhibited by a number of pharmacological agents. The first class of drugs shown to demonstrate this property was the phenothiazines (Levin & Weiss, 1976), although many drugs of other pharmacological classes are known to interact with CaM in the presence of calcium and prevent its stimulatory effects (Roufogalis *et al.*, 1983; Van Belle, 1984; Prozialeck & Weiss, 1982). One of the strongest inhibitors of CaM in the phenothiazine class of drugs is trifluoperazine (TFP). In order to understand the structural basis for binding of drugs and especially phenothiazines to calmodulin, we have crystallized a 1:1 complex of CaM and TFP and determined the X-ray structure at 2.45-Å resolution.

EXPERIMENTAL PROCEDURES

Crystals of a CaM−TFP complex have been reported by two different groups, using similar conditions and techniques (Kawasaki *et al.*, 1985; Gehrig *et al.*, 1984). For our initial studies, the CaM−TFP complex was prepared by making a solution of 0.87 mM bovine brain CaM, 10.0 mM $CaCl_2$, and 4.0 mM TFP (Kawasaki *et al.*, 1985). (TFP was from Sigma Chemical Co., St. Louis, MO.) Screening around the published conditions, using the hanging drop technique, produced poor crystals similar to those reported. However, better crystals were grown at 4 °C by vapor diffusion in hanging drops (2 μL) containing 1 μL of CaM−TFP solution mixed with 1 μL of 20% poly(ethylene glycol) monomethyl ether 2000 (PEG-MME 2000) and 0.1 M sodium cacodylate, pH 5.8. The wells contained 1 mL of 20% PEG-MME 2000 in the same buffer.

Intensity data were collected at 22 °C with a Nicolet X-100A area detector using Cu Kα radiation from a Rigaku RU-300 rotating anode generator operating at 40 kV and 100 mA. For the initial X-ray studies, two data sets were collected from one crystal. The detector-to-crystal distance was 24 cm, and the detector 2θ value was 21°. Oscillation frames covered 0.25° and were measured for 5 min. These crystals were rather thin and diffracted to a maximum resolution of about 2.6-Å resolution. Table 1 gives statistics for the data processing. Indexing and integration of intensity data were carried out using the XENGEN processing programs (Howard *et al.*, 1987).

Although space group $P3_121$ or $P3_221$ was reported by the two groups who have published crystallization conditions, we indexed the crystals without assuming that the space

[†] Supported by NIH Grants NS-30374 and CA-13148 and NASA Grant NAGW813 (W.J.C.).

[‡] The coordinates and structure factors for CaM−TFP have been deposited with the Brookhaven Protein Data Bank (Accession No. 1CTR).

* Send correspondence to this author at BioCryst Pharmaceuticals, Inc., 2190 Parkway Lake Drive, Birmingham, AL 35244 [telephone (205) 444-4605; FAX (205) 444-4640].

[§] Department of Pathology.

[||] Center for Macromolecular Crystallography.

[⊥] Department of Pharmacology.

[⊗] Abstract published in *Advance ACS Abstracts,* December 1, 1994.

[1] Abbreviations: CaM, Calmodulin; TFP, trifluoperazine; CAPP, 2-chloro-10-(3-aminopropyl)phenothiazine; $CAPP_1$−CaM, covalent adduct of 1 mol of norchlorpromazine isothiocyanate with 1 mol of calmodulin.

0006-2960/94/0433-15259$04.50/0

Table 1: Summary of Data Collection for the CaM−TFP Complex[a]

data	resolution (Å)	observations (no.)	unique (no.)	R_{sym}
native no. 1	2.65	20493	5133 (93)	8.3
native no. 2	2.45	16284	6240 (89)	9.2
$Pb(C_2H_3O_2)_2$	3.0	9305	3469 (90)	6.8
K_2PtCl_4	3.0	9686	3728 (96)	8.8

[a]The crystals used for native no. 1 and the two heavy-atom derivatives were grown from solutions containing 4 mM TFP. The crystal used for native no. 2 was grown from a solution containing 10 mM TFP. The number in parentheses after the number of unique reflections is the percent completeness of the data. R_{sym} is defined as $\sum_h \sum_{i=1}^{N} |\bar{I}(h) - I(h)_i| / \sum_h \sum_{i=1}^{N} I(h)_i$, where $I(h)_i$ is the ith measurement of reflection h and $\bar{I}(h)$ is the mean value of the N equivalent reflections.

group would be the same. Of the potential solutions generated by the indexing program, one had angles and axial lengths that were very close to the reported values and was the only solution that successfully indexed all reflections. The cell parameters refined to $a = b = 40.8$ Å and $c = 177.0$ Å. Comparison of the integrated intensities of potentially equivalent reflections based on Laue symmetry $3m$ ($\bar{3}m1$ or $\bar{3}1m$) and $6/m$ confirmed the point group symmetry $\bar{3}m1$. The systematic absence of reflections $00l$ with $l \neq 3n$ indicated either space group $P3_121$ or its enantiomorph $P3_221$. For a molecular weight of 17 273 (1:1 complex), the calculated value of V_m (Matthews, 1968) for six molecules per cell is 2.46 Å^3/Da, which is in the usual range for proteins. Thus, there is one CaM−TFP complex in the asymmetric unit, and the solvent volume fraction is about 50%.

The crystal structure was solved using a combination of molecular replacement and multiple-isomorphous-replacement (MIR) techniques. Initially, we used the molecular replacement routines in X-PLOR (Brünger, 1992). Search models for the N- and C-terminal domains consisted of residues 5−74 and 85−147 from the 1.7-Å crystal structure of CaM (Chattopadhyaya *et al.*, 1992). Cross-rotation functions were calculated using data between 12- and 4-Å resolution and a radius of integration of 21 Å. All of the peaks from each rotation search were subjected to Patterson correlation (PC) refinement (Brünger, 1990), treating the entire N- or C-terminal domain as a rigid body.

Translation functions were calculated for the top 10 PC-refinement solutions for each domain, using data from 12- to 4-Å resolution for each of the enantiomorphic space groups. With the second highest solution from the PC refinement results, the translation function for the C-terminal domain produced a clear solution. For space group $P3_221$ the highest translation function T value was 0.318 [$\sigma(T) = 0.037$] while for the corresponding rotation in space group $P3_121$ the highest value was only 0.268 [$\sigma(T) = 0.038$]. The R-factors for these solutions, using data from 8- to 4-Å resolution, were 0.519 and 0.541, respectively. On the basis of these results, the space group $P3_221$ was chosen. A similar strategy was used for the N-terminal domain, but no clear solution was obtained. In fact, the best rotation and translation solutions for the N-terminal half gave the same position as the C-terminal domain.

A $(2|F_o| - |F_c|)$ electron density map calculated with phases based on the C-terminal domain was not interpretable. Therefore, two heavy-atom derivatives [K_2PtCl_4 and $Pb(C_2H_3O_2)_2$] were prepared by soaking crystals for 24 h at 4 °C in 30% PEG-MME solutions at pH 5.8 and 0.1 M sodium cacodylate. The concentrations for the Pt and Pb compounds were 1 and 1.5 mM, respectively. Intensity data for the derivative crystals were collected using the same conditions as the native, except that the detector 2θ value was 18°. Heavy-atom positions were determined by difference Fourier maps calculated with phases based on the partial model. Cross difference Fourier maps were used in conjunction with the anomalous data to verify the choice of space group $P3_221$. The heavy atom sites were refined by least squares analysis using data from the centric zones. Table 2 gives statistics for the heavy-atom derivatives. Heavy-atom refinement, MIR phase calculations, and phase combination were done with the CCP4 package of programs (CCP4 Program Suite, Daresbury Laboratories, Daresbury, England).

Using the heavy-atom derivatives, the overall figure of merit was 0.53 for the complete data set to 3.0-Å resolution. The map was of moderate quality, but it showed seven of the eight α-helices in CaM. The N-terminal domain was placed in the density and fit as a rigid body by visual inspection, using the graphics program FRODO (Jones, 1978). Electron density maps calculated with MIR phases combined with the partial model phases were used to model residues 1−4 and 81−84. There is no significant electron density for residues 75−80 or for Lys148 at the C-terminus.

Refinement was by simulated annealing using X-PLOR (Brünger, 1992), alternating with manual rebuilding using the computer program FRODO (Jones, 1978). Difference electron density maps calculated with coefficients $(2|F_o| - |F_c|)$ or $(|F_o| - |F_c|)$ and α_c phases from the refined 2.65-Å resolution structure were used to identify the position of a TFP molecule in the C-terminal domain of CaM. No density corresponding to any other TFP molecules was identified. However, the density for this single TFP molecule was poor, and the drug molecule did not refine very well. Therefore, we decided to try to increase the occupancy by using a higher concentration of TFP in the crystallization solution. The concentration of TFP in the crystallization solution was increased to 10 mM, but all other conditions remained the same, and crystals of similar quality were grown. Two X-ray data sets were collected from one of these crystals. The detector-to-crystal distance was 24 cm, and the detector 2θ value was 24°. This crystal was slightly better than the original crystals, and data to 2.45-Å resolution were collected (Table 1). The cell parameters for this crystal were slightly larger with $a = b = 41.0$ Å and $c = 178.9$ Å.

Using this higher resolution data, $(2|F_o| - |F_c|)$ and $(|F_o| - |F_c|)$ maps were calculated, and they showed the electron density for the TFP molecule bound to the C-terminal domain quite clearly (Figure 1). However, there was still no other electron density to suggest that additional TFP molecules might be present. Using the published coordinates of TFP (McDowell, 1980), the drug molecule was fit to the density. After two more rounds of simulated annealing and model building, individual thermal parameters were introduced with restraints on the differences of temperature factors between connected atoms. Difference Fourier maps were examined for the water molecules typically found coordinated to the Ca^{2+} ion in EF hands, but no well-defined density cor-

Table 2: Refinement of Heavy-Atom Derivatives at 3.0-Å Resolution[a]

data	R_F	binding site	relative occupancy	x	y	z	R_{cen}	F_H/E
$Pb(C_2H_3O_2)_2$	17.2	EF hand 1	0.185	0.604	0.238	0.561	58.5	1.5
		EF hand 2	0.029	0.332	0.090	0.519		
K_2PtCl_4	17.4	Met145	0.123	0.244	0.499	0.589	56.1	1.4
		Met36, Met51	0.129	0.282	0.226	0.609		
		Met71, Met72	0.068	0.266	0.375	0.564		

[a] R_F is the percentage change between native (F_1) and scaled derivative (F_2) data ($\sum||F_1| - |F_2||/\sum|F_1|$). R_{cen} is the centric R value [$(\sum|F_{H(o)} - F_{H(c)}|)/\sum|F_{H(o)}|$] for the heavy-atom refinement. F_H/E is the average value of the heavy-atom contribution divided by lack-of-closure error. Heavy-atom refinement, MIR phase calculations, and phase combination were done with the CCP4 package of programs (Daresbury Laboratories, Daresbury, England).

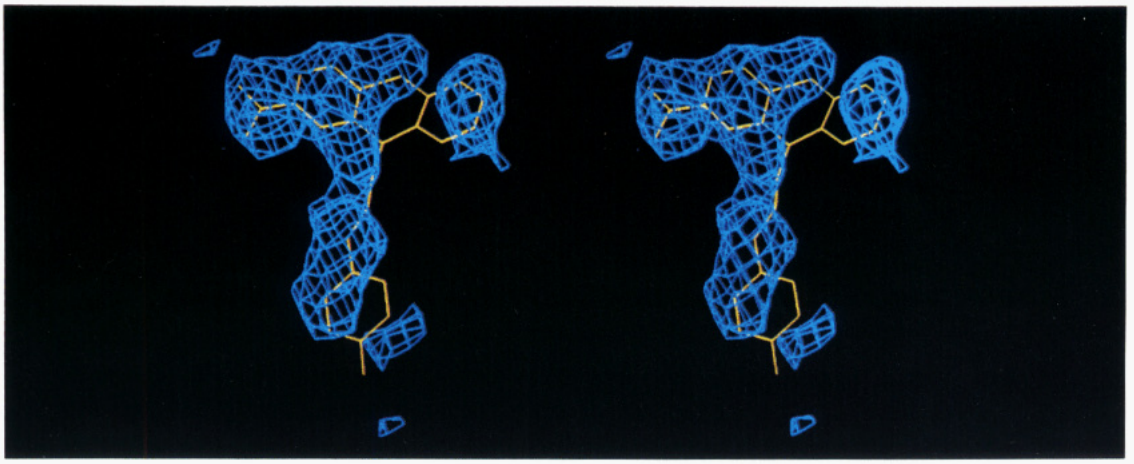

FIGURE 1: TFP with the superimposed difference electron density contoured at 1.0σ. The electron density map was calculated with coefficients ($|F_o| - |F_c|$) and α_c phases from the refined 2.45-Å resolution structure of CaM only. Figures 1, 2, and 4 were prepared with CHAIN (Sack, 1988).

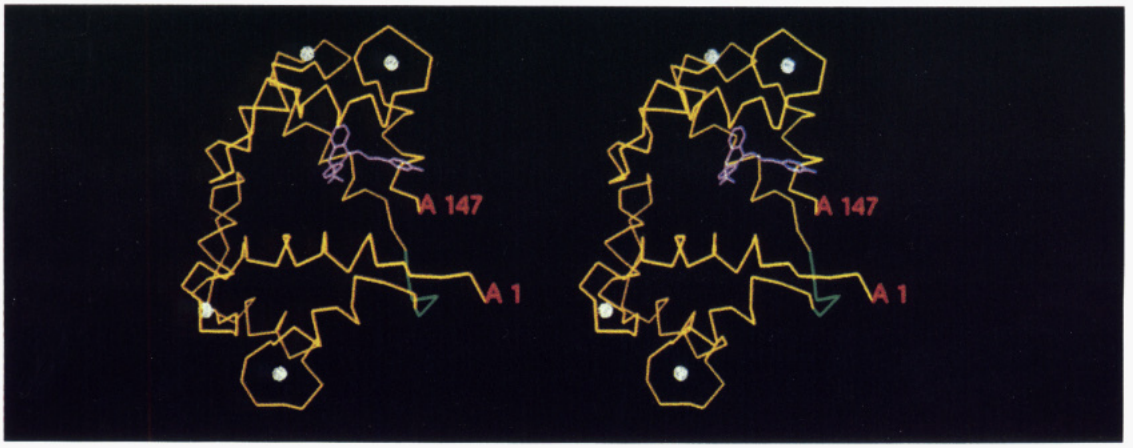

FIGURE 2: Stereo drawing of the α-carbon backbone trace of CaM (yellow) and TFP (magenta). The four Ca^{2+} atoms are shown as spherical dot surfaces. The strand of residues 75−80 (green), which divides the central helix of native CaM into two helices (IV and V) in the CaM−TFP complex, has very little electron density in the MIR and ($2|F_o| - |F_c|$) maps. The model of this strand (which is also used in Figure 4) is based on the corresponding region in the CaM−skMLCK peptide structure (Ikura *et al.*, 1992). The last residue of CaM (Lys148) has no density and is not shown.

responding to solvent was identified. No attempt was made to search for other solvent molecules. The final model includes 141 residues (1−74 and 81−147) with 1109 protein atoms, 4 Ca^{2+} ions, and 1 TFP. The R-factor, based on 5060 reflections in the range 2.45 Å ≤ d ≤ 6.0 Å with $F > 2\sigma(F)$, is 0.222. The estimated error in atomic coordinates is 0.3 Å (Luzzati, 1952). Root-mean-square deviations from ideality are 0.015 Å for bond distances and 2.5° for angles.

RESULTS

The structure of the CaM−TFP complex is shown in Figures 2 and 3. The most remarkable feature of the structure is the marked similarity to the structure of CaM in CaM−peptide complexes (Ikura *et al.*, 1992; Meador *et al.*, 1992, 1993) (Figure 3). Although residues 75−80 could not be identified, there is obviously a sharp bend at this position in the α-helix that connects the N- and C-terminal domains, thus producing two α-helices comprising residues 65−72 and 83−92. A similar distortion in the central helix was seen in the crystal and NMR structures of CaM−peptide complexes. It is noteworthy that in all three of those structures the residues in this region were either invisible or very poorly defined, suggesting that they are extremely flexible and/or disordered.

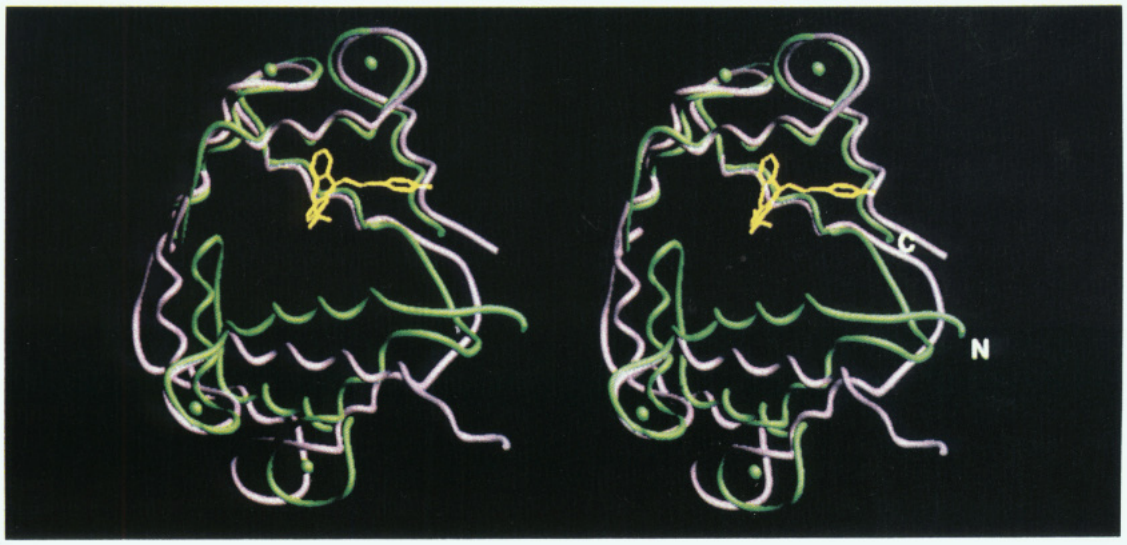

FIGURE 3: Stereo model of CaM (green) complexed with TFP (yellow) superimposed on CaM from the CaM−skMLCK peptide complex (magenta). The orientation is approximately the same as in Figure 2. The superposition is based on the Cα positions for residues 81−147 from the C-terminal domains. The four Ca^{2+} atoms from the CaM−TFP structure are shown as spheres. This figure was prepared with RIBBONS (Carson, 1987).

The two domains of CaM in the complex are similar, even though only one domain has a bound TFP. Superimposition of residues 8−74 onto residues 81−147 shows a root-mean-square deviation of 0.8 Å for α-carbon atoms. The only close contacts (<4 Å) between the N- and C-terminal domains involve helices I and II of the N-terminal domain with helices V and VI of the C-terminal domain. The pseudo-2-fold symmetry noted in the three structures of CaM−peptide complexes (Ikura *et al.*, 1992; Meador *et al.*, 1992, 1993) is also present in CaM−TFP, but the symmetry is less exact. The two domains in CaM−TFP are related by an angle of 172°, whereas in the CaM−skMLCK peptide complex the angle is 179°.[2] This rotation allows helix I in the N-terminal domain to assume a position that helps shield the TFP molecule from solvent (Figure 3). The molecule is more compact than the CaM in either of the CaM−MLCK structures, with overall dimensions of about 30 × 32 × 42 Å, compared to 30 × 32 × 47 Å for skMLCK. Certain helices around the TFP binding site show especially large movements. For example, the distance between Glu11 and Glu120 decreases by 7 Å, while the distance between Glu11 and Met145 increases by about 2 Å.

Thirteen residues form 191 contacts (<5 Å) between CaM and TFP (Table 3). Only one of these residues (Glu11) is furnished by the N-terminal domain. Ten of the residues are hydrophobic; the other three are Glu residues, but they form only van der Waals contacts. The tricyclic ring of TFP lies in the same hydrophobic pocket in the C-terminal domain that is utilized in binding peptides (Figure 4). In the three CaM−peptide complexes that have been reported, the residue occupying this site is Trp in the two MLCK polypeptides and Leu in the kinase polypeptide. In fact, a number of studies have shown that a large hydrophobic residue in this position, usually Trp, is required for high affinity of substrate enzymes to CaM (Bagchi *et al.*, 1992; O'Neil *et al.*, 1989; VanBerkum & Means, 1991). All five of the residues that make contacts with the Trp residue in the CaM−smMLCK peptide complex also make contacts with the tricyclic ring of TFP. The ring lies between the side chains of Met124 and Met144, with the most extensive contacts involving Met124. The tricyclic ring and the side chains of Phe92 and Phe141, which are almost mutually perpendicular to each other, form an aromatic cluster. The three-carbon linker between the tricyclic ring and the piperazine ring is almost fully extended. The piperazine ring, which has a net positive charge, lies between several hydrophobic residues and is close to a cluster of glutamate residues formed by the juxtaposition of the two domains. This part of TFP is in the same vicinity as the basic residues proximal to Trp in the MLCK polypeptide, although it is relatively closer to the C-terminal domain. There are no salt bridges between the N atoms of the ring and carboxylate oxygen atoms from acidic residues.

Table 3: Contacts between TFP and CaM (<5.0 Å)

TFP moiety	residue	no. of contacts	minimum distance (Å)	maximum distance (Å)
tricyclic ring	Phe92	5	4.23	4.98
	Ile100	4	3.88	4.95
	Leu105	8	3.74	4.95
	Met109	2	4.79	4.95
	Met124	25	3.65	4.99
	Ile125	6	4.53	4.95
	Glu127	1	4.80	4.80
	Ala128	6	3.39	4.82
	Val136	8	3.77	4.78
	Phe141	4	4.63	4.84
	Met144	20	3.52	4.81
CF_3 group	Glu11	12	3.86	4.96
	Glu123	4	3.65	4.95
	Met124	7	3.54	4.80
	Glu127	4	4.14	4.96
aliphatic chain	Met124	6	3.37	4.97
	Glu127	10	3.82	4.82
	Ala128	9	3.37	4.34
	Met144	9	3.40	4.77
piperazine ring	Glu127	10	4.11	4.97
	Ala128	8	3.65	4.73
	Met144	23	3.07	4.93

One of the most surprising features of the complex is that only one molecule of TFP is bound to CaM. Most chemical and spectroscopic studies have predicted that CaM has two

[2] The coordinates for the two X-ray structures by Meador *et al.* (1992, 1993) are not available, so no direct comparison is possible.

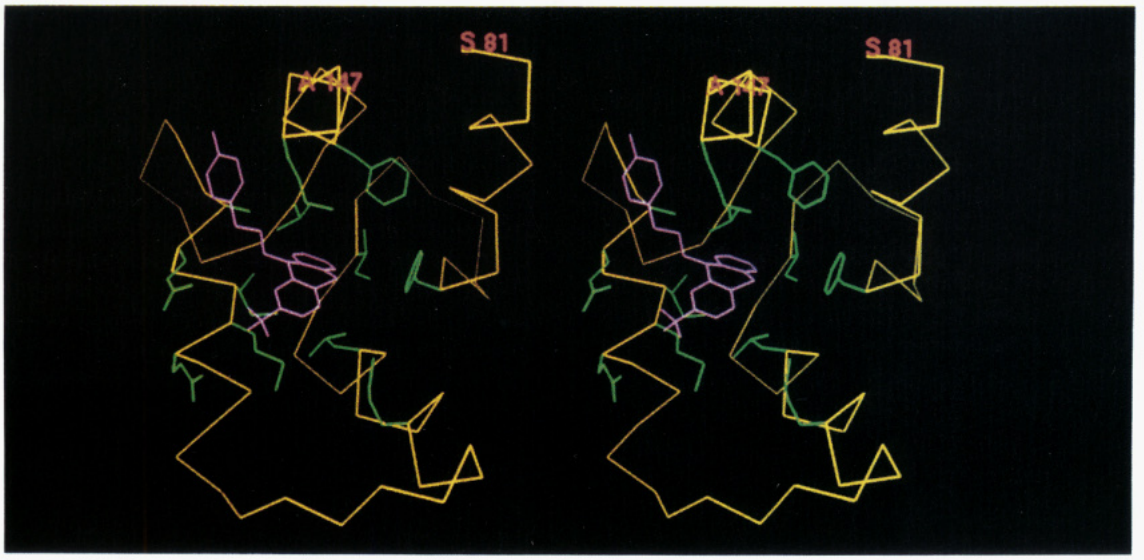

FIGURE 4: Stereo drawing of TFP (magenta) and its environment in the C-terminal domain of CaM (yellow). Side chains within 5 Å of TFP are shown (green).

high-affinity binding sites (Dalgarno *et al.*, 1984; Krebs & Carafoli, 1982; Klevit *et al.*, 1981; Thulin *et al.*, 1984; Faust *et al.*, 1987). However, using HPLC, Kawasaki *et al.* (1985) determined that the TFP−CaM molar ratio in their crystals was 1.1 ± 0.1. Since our initial crystallization conditions were similar to theirs, we suspected that our complex might contain only one TFP molecule. After our initial studies showed only one TFP molecule in the complex, we increased the ratio of TFP to CaM from 4.5:1 to 11.5:1 and grew crystals under the same conditions. Using a contour level of 1.0σ for the difference electron density maps, the electron density for the TFP molecule bound to the C-terminal domain became even clearer than before, but there was still only random noise in the analogous region of the N-terminal domain. Furthermore, no significant electron density was identified in any other region of calmodulin. By superimposing the C-terminal domain containing the bound TFP onto the N-terminal domain, we were able to identify the corresponding hydrophobic pocket in the N-terminal domain. However, after refinement there was still no well-defined electron density for the second TFP molecule in the $(2|F_o| - |F_c|)$ map. Therefore, it seems very unlikely that more than one TFP molecule is bound to calmodulin in our structure.

It is not clear why no TFP is bound to the N-terminal domain, although one possible explanation is the difference in pH between our conditions for crystal growth (pH 5.8) and the pH used in spectroscopic studies, which ranged from 7.0 to 7.5 (Dalgarno *et al.*, 1984; Krebs & Carafoli, 1982; Klevit *et al.*, 1981; Thulin *et al.*, 1984). The hydrophobic pockets in the N- and C-terminal domains have 71% sequence identity, and all but two of the residues in the C-terminal domain that form contacts with TFP have identical residues in homologous positions in the N-terminal domain. In those two cases, Ala128 and Val136 would be replaced by Val55 and Ile63, respectively. Both of these residues have larger side chains, which could cause steric problems and result in a lower binding affinity. The counterpart to the sole residue contributed by the N-terminal domain (Glu11) would be Glu84. However, in the crystal structure, it would be at least 1−2 Å further away from TFP. The major difference in these two sites is the lack of residues for electrostatic interactions with the piperazine ring. The cluster of glutamate residues adjacent to the TFP binding site in the C-terminal domain has no counterpart for the putative binding site in the N-terminal domain. It is worth noting that Thulin *et al.* provided evidence that the TFP binding site in the C-terminal domain has a higher affinity for the drug than the binding site in the N-terminal half (Thulin *et al.*, 1984).

DISCUSSION

There are at least two essential structural features of CaM-binding drugs (Prozialeck & Weiss, 1982). The first is a large hydrophobic region, consisting of two or three aromatic rings. From an examination of the hydrophobic binding pocket, this requirement is readily explained. The size and shape of the pocket will accommodate a bulky hydrophobic group, and the two Phe residues adjacent to the pocket can form aromatic−aromatic interactions. The second required feature is a positively charged amino group that is at least three atoms removed from the ring structure. Prozialeck and Weiss (1982) did not find a high degree of specificity in the type of side-chain amino group needed for a compound to inhibit CaM, although the distance between the amino group and the phenothiazine nucleus appeared to be important. In their experiments, increasing the distance from two to four carbons enhanced potency (Prozialeck & Weiss, 1982). On the basis of the crystal structure, one would predict that the presence of a positively charged group is important for interaction with the cluster of glutamate residues supplied by helices I and VII. Additional hydrophobic substituents adjacent to the charged group might allow more interactions with CaM and thus strengthen the interaction. Also, on the basis of the distance from the hydrophobic binding pocket to the Glu residues, the structure suggests that more interactions between the charged group and CaM are possible if the aliphatic chain contains at least three carbon atoms.

A number of chemical and spectroscopic studies support this model of binding for the C-terminal domain, even though most investigators have assumed that CaM maintains its dumbbell shape and has one high-affinity binding site for the drug in each globular domain. For example, a number

of investigators have used various techniques to show that Lys148 is close to the TFP binding site (Faust *et al.*, 1987; Giedroc *et al.*, 1985; Jackson & Puett, 1984). Although there was no significant electron density for Lys148 in difference Fourier maps, its approximate position can be inferred on the basis of the position of Ala147. This would place it less than 12 Å from the piperazine ring of TFP. Nuclear magnetic resonance studies have shown that TFP binding to CaM affects Met and Phe residues, especially the methionine-rich regions immediately following Ca^{2+}-binding loops 2 and 4 (Krebs & Carafoli, 1982; Klevit *et al.*, 1981). Furthermore, by using the CaM fragment 107−148, Dalgarno *et al.* (1984) showed that as TFP binds to CaM, it shifts the resonances of Met109, Met124, Met144, and Met145, as well as the resonance of Phe141. This is consistent with the crystal structure; the side chains of these residues are all part of the hydrophobic pocket in the C-terminal domain, and Met124, Met144, and Phe141 make van der Waals contacts with TFP.

It appears that hydrophobic interactions play the major role in stabilizing the bent structure of CaM−TFP. On the basis of the structures of CaM−peptide complexes, Ikura *et al.* (1992) and Meador *et al.* (1993) suggested that at least two hydrophobic residues separated by 8−12 residues were required to serve as anchors for the peptide to the N- and C-terminal hydrophobic patches of CaM. A similar suggestion was made by Kataoka *et al.* (1991), who used small-angle X-ray scattering to study the interaction between CaM and two synthetic peptides. They showed that a peptide that stopped just short of the second hydrophobic residue in CaM-binding peptides bound only to the C-terminal domain and did not significantly alter the extended structure of CaM, while a longer peptide formed a globular structure with CaM. However, the CaM−TFP structure demonstrates that while two hydrophobic residues separated by 8−12 residues may be sufficient to cause CaM to change from a dumbbell shape to a more globular shape, they are not necessary. Instead, the structure of CaM is profoundly altered upon binding of a single small molecule to the C-terminal domain.

The binding and activation of smMLCK by CaM have been studied extensively. Several lines of evidence have suggested that a Trp residue of MLCK is required for initiation of CaM binding (O'Neil *et al.*, 1989; VanBerkum & Means, 1991). Using mutant CaMs as probes, VanBerkum and Means (1991) predicted that the C-terminal portion of CaM contains the primary binding site for smMLCK, although they speculated that activation could occur only if the N-terminal domain is also present. The structure of CaM−TFP has now shown that TFP is bound in the same hydrophobic pocket as the Trp residue in the smMLCK and skMLCK peptides (Ikura *et al.*, 1992; Meador *et al.*, 1992, 1993). Thus, insertion of a large hydrophobic aromatic molecule is sufficient to cause structural changes in CaM similar to those produced by binding peptides. On the basis of the CaM−TFP structure, we would agree with VanBerkum and Means (1991) that binding of Trp or another large hydrophobic residue by the C-terminal domain of CaM is the initiating event for CaM binding to smMLCK and the subsequent conformational changes in CaM that allow enzyme activation.

It has been proposed that smMLCK is autoinhibited by a pseudosubstrate sequence binding to the active site of the enzyme (Kemp *et al.*, 1987). The CaM-binding region of smMLCK overlaps with the sequence that functions as a pseudosubstrate inhibitor of the enzyme. CaM binding displaces the substrate inhibitory domain from the active site to allow light chain phosphorylation. Direct support for the intrasteric mechanism of smMLCK regulation has been provided by the recent structure of a recombinant fragment of twitchin kinase that contains the catalytic core and a 60-residue C-terminal tail (Hu *et al.*, 1994). The C-terminal tail of twitchin kinase, which is homologous to the pseudosubstrate sequence in smMLCK, extends through the active site and makes extensive contacts with the catalytic core. Taken together, these results suggest that, in the case of smMLCK, CaM binds initially through its C-terminal domain to the CaM-binding domain, but activation only occurs when the N-terminal domain also binds to the enzyme and thus "pulls" the pseudosubstrate away from the active site.

The ability of CaM to undergo such a dramatic conformational change upon binding of substrate to only one domain has implications for the mechanism of enzyme activation by CaM in general. Newton *et al.* (1983) have described a covalent adduct of CaM with one molecule of phenothiazine ($CAPP_1$−CaM), in which the phenothiazine reacts with Lys75. These investigators subsequently showed that the $CAPP_1$−CaM will interact with various CaM-dependent enzymes with a relatively high affinity but either does not activate the enzyme (smMLCK and phosphodiesterase) (Newton & Klee, 1984), activates the enzyme only partially (calcineurin) (Newton & Klee, 1984), or acts as a full agonist (glycogen synthase kinase and phosphorylase kinase) (Newton *et al.*, 1985). From these results, it appears that occupancy of the phenothiazine-binding site in the N-terminal domain of CaM has little effect on its affinity for all enzymes tested, but has a pronounced effect on its ability to activate some enzymes under its control. On the basis of the crystal structure, as well as the results noted above, we would predict that the C-terminal domain of CaM contains the primary recognition site for most CaM-dependent enzymes. Furthermore, in the case of smMLCK, we suspect that the reason $CAPP_1$−CaM prevents activation is because the N-terminal domain is unable to interact with the enzyme and remove the pseudosubstrate from the active site.

NOTE ADDED IN PROOF

After submission of this paper, an article appeared describing the crystal structure of a CaM−TFP complex (Vandonselaar *et al.*, 1994). Although the two structures appear similar overall, the Vandonselaar structure contains four TFP molecules complexed with CaM, as opposed to the one TFP molecule seen in our structure. TFP1 in their structure corresponds to our sole TFP molecule in the C-terminal domain of CaM. However, the phenothiazine moiety has been inverted with respect to the published structure (McDowell, 1980), and it has also been rotated 180° with respect to our structure, placing the trifluoro moiety close to Val136. The other three TFP molecules reported by Vandonselaar *et al.* are of much lower occupancy with very high mean temperature factors, especially the TFP molecule in the N-terminal domain. Although their coordinates are not available to us, making a direct comparison impossible, we do note small pieces of poorly defined electron density in our final $(2|F_o| - |F_c|)$ map in the regions of these additional TFP molecules. Whether this electron density represents additional *bona fide* TFP molecules is not clear, but we think it is unlikely. In this regard, it is

important to reiterate that Kawasaki *et al.* (1985) determined that the TFP−CaM molar ratio was 1.1 ± 0.1 in crystals grown under the conditions we initially used. Finally, the ratio of TFP to CaM in our original crystallization mixture was 4.5:1, as opposed 35:1 in the conditions reported by Vandonselaar *et al.* It is possible that additional TFP molecules may bind nonspecifically with very low occupancy at such high molar ratios of TFP to CaM.

ACKNOWLEDGMENT

We thank Anthony R. Means and Y. S. Babu for critical review of the manuscript prior to submission, Sonia R. Anderson for purified calmodulin, and Brent Cole for assistance with photography.

REFERENCES

Babu, Y. S., Bugg, C. E., & Cook, W. J. (1988) *J. Mol. Biol. 204*, 191−204.

Bagchi, I. C., Huang, Q., & Means, A. R. (1992) *J. Biol. Chem. 267*, 3024−3029.

Brünger, A. T. (1990) *Acta Crystallogr., Sect. A 46*, 46−57.

Brünger, A. T. (1992) *X-PLOR Version 3.0*, Yale University, New Haven, CT.

Carson, M. (1987) *J. Mol. Graphics 5*, 103−106.

Chattopadhyaya, R., Meador, W. E., Means, A. R., & Quiocho, F. A. (1992) *J. Mol. Biol. 228*, 1177−1192.

Dalgarno, D. C., Klevit, R. E., Levine, B. A., Scott, G. M. M., Williams, R. J. P., Gergely, J., Grabarek, Z., Leavis, P. C., Grand, R. J. A., & Drabikowski, W. (1984) *Biochim. Biophys. Acta 791*, 164−172.

Faust, F. M., Slisz, M., & Jarrett, H. W. (1987) *J. Biol. Chem. 262*, 1938−1941.

Gehrig, L. M. B., Delbaere, L. T. J., & Hickie, R. A. (1984) *J. Mol. Biol. 177*, 559−561.

Giedroc, D. P., Sinha, S. K., Brew, K., & Puett, D. (1985) *J. Biol. Chem. 260*, 13406−13413.

Howard, A. J., Gilliland, G. L., Finzel, B. C., Poulos, T. L., Ohlendorf, D. H., & Salemme, F. R. (1987) *J. Appl. Crystallogr. 20*, 383−387.

Hu, S.-H., Parker, M. W., Lei, J. Y., Wilce, M. C. J., Benian, G. M., & Kemp, B. E. (1994) *Nature 369*, 581−584.

Ikura, M., Clore, G. M., Gronenborn, A. M., Zhu, G., Klee, C. B., & Bax, A. (1992) *Science 256*, 632−638.

Jackson, A. E., & Puett, D. (1984) *J. Biol. Chem. 259*, 14985−14992.

Jones, T. A. (1978) *J. Appl. Crystallogr. 11*, 268−272.

Kataoka, M., Head, J. F., Vorherr, T., Krebs, J., & Carafoli, E. (1991) *Biochemistry 30*, 6247−6251.

Kawasaki, H., Itoh, S., Kasai, H., Mitsui, Y., IItaka, Y., Nakanishi, M., & Okuyama, T. (1985) *J. Biochem. 97*, 1815−1818.

Kemp, B. E., Pearson, R. B., Guerriero, V., Jr., Bagchi, I. C., & Means, A. R. (1987) *J. Biol. Chem. 262*, 2542−2548.

Klee, C. B., & Vanaman, T. C. (1982) *Adv. Protein Chem. 35*, 213−321.

Klevit, R. E., Levine, B. A., & Williams, R. J. P. (1981) *FEBS Lett. 123*, 25−29.

Krebs, J., & Carafoli, E. (1982) *Eur. J. Biochem. 124*, 619−627.

LaPorte, D. C., Wierman, B. M., & Storm, D. R. (1980) *Biochemistry 19*, 3814−3819.

Levin, R. M., & Weiss, B. (1976) *Mol. Pharmacol. 12*, 581−589.

Luzzati, V. (1952) *Acta Crystallogr. 5*, 802−810.

Matthews, B. W. (1968) *J. Mol. Biol. 33*, 491−497.

McDowell, J. J. H. (1980) *Acta Crystallogr. B36*, 2178−2181.

Meador, W. E., Means, A. R., & Quiocho, F. A. (1992) *Science 257*, 1251−1255.

Meador, W. E., Means, A. R., & Quiocho, F. A. (1993) *Science 262*, 1718−1721.

Means, A. R., VanBerkum, M. F. A., Bagchi, I., Lu, K. P., & Rasmussen, C. D. (1991) *Pharmacol. Ther. 50*, 255−270.

Newton, D. L., & Klee, C. B. (1984) *FEBS Lett. 165*, 269−272.

Newton, D. L., Burke, T. R., Jr., Rice, K. C., & Klee, C. B. (1983) *Biochemistry 22*, 5472−5476.

Newton, D. L., Klee, C. B., Woodgett, J., & Cohen, P. (1985) *Biochim. Biophys. Acta 845*, 533−539.

O'Neil, K. T., Erickson-Viitanen, S., & DeGrado, W. F. (1989) *J. Biol. Chem. 264*, 14571−14578.

Prozialeck, W. C., & Weiss, B. (1982) *J. Pharmacol. Exp. Ther. 222*, 509−516.

Roufogalis, B. D., Minocherhomjee, A. M., & Al-Jobore, A. (1983) *Can. J. Biochem. Cell Biol. 61*, 927−933.

Sack, J. S. (1988) *J. Mol. Graphics 6*, 224−225.

Tanaka, T., & Hidaka, H. (1980) *J. Biol. Chem. 255*, 11078−11080.

Thulin, E., Andersson, A., Drakenberg, T., Forsén, S., & Vogel, H. J. (1984) *Biochemistry 23*, 1862−1870.

Van Belle, H. (1984) in *Advances in Cyclic Nucleotide and Protein Phosphorylation Research* (Greengard, P., *et al.*, Eds.) Vol. 17, pp 557−567, Raven Press, New York.

VanBerkum, M. R. A., & Means, A. R. (1991) *J. Biol. Chem. 266*, 21488−21495.

Vandonselaar, M., Hickie, R. A., Quail, J. W., & Delbaere, L. T. J. (1994) *Nature Struct. Biol. 1*, 795−801.

Vogel, H. J., Lindahl, L., & Thulin, E. (1983) *FEBS Lett. 157*, 241−246.